HHS Public Access

Author manuscript

Lasers Med Sci. Author manuscript; available in PMC 2022 October 26.

Published in final edited form as:

Lasers Med Sci. 2013 July ; 28(4): 1143–1150. doi:10.1007/s10103-012-1202-4.

Spatially Controlled Photothermal Heating of Bladder Tissue Through Single-Walled Carbon Nanohorns Delivered with the Fiberoptic Microneedle Device

R. Lyle Hood[1], **William F. Carswell**[1], **Amanda Rodgers**[1], **Mehmet A. Kosoglu**[2], **M. Rylander**[1,2], **David Grant**[3], **John L. Robertson**[3], **Christopher G. Rylander**[1,2]

[1]School of Biomedical Engineering and Sciences Virginia Tech, Blacksburg, VA 24061

[2]Department of Mechanical Engineering Virginia Tech, Blacksburg, VA 24061

[3]Virginia-Maryland Regional College of Veterinary Medicine Virginia Tech, Duck Pond Drive, Blacksburg, VA 24061

Abstract

Laser-based photothermal therapies for urothelial cell carcinoma (UCC) are limited to thermal ablation of superficial tumors, as treatment of invasive lesions is hampered by shallow light penetration in bladder tissue at commonly used therapeutic wavelengths. This study evaluates the utilization of sharp, silica, fiberoptic microneedle devices (FMDs) to deliver single-walled carbon nanohorns (SWNHs) serving as exogenous chromophores in conjunction with a 1064 nm laser to amplify thermal treatment doses in a spatially controlled manner. Experiments were conducted to determine the lateral and depth dispersal of SWNHs in aqueous solution (0.05 mg/mL) infused through FMDs into the wall of healthy, inflated, *ex vivo* porcine bladders. SWNH perfused bladder regions were irradiated with a free-space, CW, 1064 nm laser in order to determine the SWNH efficacy as exogenous chromophores within the organ. SWNHs infused at a rate of 50 μL/min resulted in an average lateral expansion rate of 0.36 ± 0.08 cm^2/min. Infused SWNHs dispersal depth was limited to the urothelium and muscular propria for 50 μL/min infusions of 10 minutes or less, but dispersed through the entire thickness after a 15 minute infusion period. Irradiation of SWNH perfused bladder tissue with 1064 nm laser light at 0.95 W/cm^2 over 40 seconds exhibited a maximum increase of approximately 19°C compared with an increase of approximately 3°C in a non-perfused control. The results indicate that these silica FMDs can successfully penetrate into the bladder wall to rapidly distribute SWNHs with some degree of lateral and depth control and that SWNHs may be a viable exogenous chromophore for photothermal amplification of laser-based UCC treatments.

Keywords

Microfluidics; Bladder Cancer; Biotransport; Exogenous Chromophores; Microneedles

Correspondence should be sent to: Christopher G. Rylander, 325 ICTAS Bldg. Stanger St. (0298), Blacksburg, VA, 24061, Office: (540)231-0964, Fax: (540)231-9738, cgr@vt.edu.

1.0 Background and Objectives

Urinary bladder cancer is the fourth most common non-cutaneous malignancy of humans in the United States with approximately 71,000 new cases diagnosed and 15,000 deaths in 2010 [1]. Urothelial cell carcinoma (UCC, synonymous with transitional cell carcinoma) accounts for approximately 90% of all bladder cancers. Over 30% of UCCs are at an advanced clinical stage when diagnosed, with penetration of tumor cells into the muscularis propria (stages 3 and 4), serosa (stage 4 only), and metastasis to surrounding organs [2–4]. Radical cystectomy of invasive UCC is the current standard treatment, but its use frequently results in significant post-operative complications and poor patient quality of life [5]. This treatment typically requires removal of the bladder, nearby lymph nodes, and part of the urethra in both sexes; the prostate, seminal vesicles, and vas deferens in men; and the ovaries, fallopian tubes, and part of the vagina in women [5–7]. This treatment often results in sexual dysfunction, electrolyte imbalances, bone loss, and deterioration of the kidneys [8, 9]. Patients are faced with poor quality of life, bleak prognoses, and low survival rates (30–50% at 5 years post diagnosis) [2].

Although patient outcomes for advanced stage, invasive bladder cancers are statistically poor, patient outcomes for early stage (stages 0–1) bladder cancers are relatively optimistic [10–12]. The primary treatment for such early lesions is transurethral resection of the bladder (TURB) followed by chemotherapy [12–17]. TURB describes the introduction of a cystoscope through the urethra to debulk a tumor via excision, radiofrequency ablation, electrocautery (ablation through resistive heating of a wire probe), or laser ablation. The major advantages provided by laser ablation include high precision and significantly reduced bleeding [13, 18]. One of the original laser-based alternatives for treatment of superficial bladder tumors was Nd:YAG laser tissue coagulation at a 1064 nm wavelength. Unfortunately, laser energy delivered at this wavelength is highly penetrating through bladder tissue and can damage surrounding organs [10, 13, 19, 20]. Nd:YAG-based treatments were succeeded by the Ho:YAG laser (2.1 μm wavelength) for photothermal treatment of superficial bladder cancers, which has become widely utilized. Several studies have shown that treatment with the Ho:YAG laser is safe, effective, and associated with rapid patient recovery, indicating it is a viable alternative to surgical excision or electrocautery for treating early stage bladder cancer [11–13, 20].

While effective for superficial tumors, Ho:YAG laser treatment has proven ineffective for invasive, late stage bladder tumors due to insufficient light penetration into the tumor mass [11, 13, 20–22]. Light at a wavelength of 2.1 μm penetrates bladder tissue approximately 0.5 mm, which is insufficient to treat late stage tumors that invade the muscular and serosal layers 2–4 mm into the bladder wall [4, 13]. Inadequate delivery and heating of deep tumor volumes results in generation of poorly defined lesion boundaries and a high likelihood of tumor recurrence, necrosis, and possible perforation of the bladder wall [9, 23]. As 2.1 μm light is too superficial for treating more invasive tumors and 1064 nm light is too penetrating, the use of exogenous chromophores in conjunction with 1064 nm light could enable spatial control of the photothermal effect at the depths necessary for treatment of late stage neoplasms.

Single-walled carbon nanohorns (SWNHs) have recently attracted attention as photoabsorbers and intracellular delivery vehicles for therapeutic drugs and imaging moieties [24, 25]. Carbonaceous nanoparticles absorb light in the near-infrared region, and can cause cell death through photothermal hyperthermia [24]. One of the most important advantages SWNHs have over similar carbon nanoparticles is that they are produced without the use of metal catalysts, significantly lowering their cytotoxicity [26–28]. Other advantages include highly consistent particle size and a lower aspect ratio with respect to single- and multi-walled nanotubes. Additionally, SWNHs have been demonstrated to produce reactive oxygen species when heated, which implies their use may also leverage photochemical effects to destroy tumors [29, 30].

Recognizing the limitations of current laser-based treatments for bladder cancer and the therapeutic potential of some newly developed nanomaterials, this study evaluates the use of a silica fiberoptic microneedle device (FMD) for delivering SWNHs serving as exogenous chromophores in conjunction with a 1064 nm laser to selectively amplify thermal treatment doses in deeper tissue regions. The FMD technology is being developed to co-deliver laser energy and fluid agents through the hollow silica fibers, but this manuscript will be describing experiments defining the fluid delivery aspect. A literature value of 2 cm^2 for a relevant tumor area laterally across the bladder wall's surface was identified as an experimental goal for SWNH dispersal [20]. For this study, the objectives was to use the FMDs to penetrate the serosa of an *ex vivo* bladder into the muscularis and infuse a sufficient volume of SWNHs through its 150 μm bore to permeate a clinically significant area (2 cm^2) in a reasonable timeframe (10 minutes), and subsequently irradiate the infused volume with an external beam of 1064 nm light causing a significant increase in photothermal heating relative to a non-perfused volume.

2.0 Methods

2.1 *Ex Vivo* Porcine Urinary Bladders

Ex vivo urinary bladders utilized in this paper (with the exception of the experiments outlined in Section 2.3) were excised from healthy, adult, mixed breed pigs of both sexes purpose-bred for research. The bladders were harvested from freshly sacrificed animals by a veterinarian in the Virginia-Maryland Regional College of Veterinary Medicine. Pigs ranged from approximately 5–10 months of age. The experiments utilized both inflated and non-inflated bladders for determination of SWNH dispersal. Bladder inflation was used to create a consistent curvature of the bladder wall, which was effected through introduction of a 18G syringe needle through the urethra into the bladder's interior and subsequent infusion of 500–750 mL of isotonic phosphate buffered saline solution (PBS). Additionally, the exterior of the bladder was moistened at 5 minute intervals with PBS to prevent drying of the serosa that could impact the fluid dispersal properties of the bladder.

2.2 Dispersal of SWNHs Laterally Across the Bladder's Serosa

SWNHs were synthesized by the Center for Nanophase Materials Sciences at Oak Ridge National Laboratories (Oak Ridge, Tennessee) by previously described methods [31]. The SWNHs were prepared and suspended in a 1 mg/mL Pluronic F-127 (Biotium, Inc.),

as previously described, at a concentration of 0.05 mg/mL [27, 32, 33]. Other groups have demonstrated that the addition of the Pluronic does not affect the cytotoxicity or heat generation of the solution [29, 34–36]. Previous studies have demonstrated that the attenuation coefficient of 0.05 mg/mL in deionized water at 1064 nm to be approximately 2.6 cm^{-1} [27].

Silica FMDs were fabricated from TSP150375 fused flexible silica capillary tubing (Polymicro Technologies, Phoenix, AZ) with an outer diameter of 363±4 μm, an inner diameter of 150±1 μm, and a polyimide outer coating thickness of 40 μm. This capillary tubing was given a sharp, beveled, microneedle tip (see Figure 1) by manual angle-polishing with a series of aluminum oxide lapping films ranging from 5–0.5 μm grit sizes (ThorLabs, Sterling, VA).

For these experiments, an FMD was affixed within the bore of a 22G stainless steel needle and attached to a syringe containing the SWNH solution by plastic tubing. The FMD was manually inserted with gentle pressure into the serosal layer of an inflated bladder at an angle of approximately 10° from the wall's surface. The FMD was inserted a length of 1–2 cm with a final depth at the microneedle's tip of 1–2 mm. The syringe was mounted in an NE-500 syringe pump (New Era Pump Systems, Inc., Farmingdale, NY), and the flow rate was set to 50 μL/min. Infusions were conducted for 15 minutes for a total infused volume of 750 μL. Images were captured with a Canon EOS Rebel T1i/EOS 500D camera (Canon USA, Lake Success, NY) every 30 seconds beginning simultaneously with the syringe pump activation. The SWNH dispersal was traced and measured using ImageJ (NIH, Bethesda, MD) by two independent observers and averaged. Any area measurements with deviation greater than 10% were remeasured by a third observer and averaged with the previous measurements. Experiments were conducted using two bladders with two infusions each (N=4).

2.3 Dispersal of Infused SWNHs throughout the Bladder's Layers

Experiments to determine the dispersal of SWNH solution through the thickness of the bladder wall were performed by infusing SWNHs into both inflated and uninflated healthy, *ex vivo* bladders. The *ex vivo* bladders used in these experiments were harvested from healthy, adult, mixed breed pigs of both sexes approximately 7 months in age from a regional abattoir (Smithfield Foods, Inc., Smithfield, VA).

Uninflated bladders were bisected and pinned open to expose the urothelium. A set of infusions was made within a bisected bladder at the thin-walled tissue near the bladder neck, where an FMD was introduced through the urothelium at an angle of approximately 10° to a superficial depth (< 1 mm). These infusions were conducted at a flow rate of 50 μL/min for 5, 10, and 15 minutes and repeated in a second bladder (N = 2). A second set of infusions was administered within a bisected and pinned bladder at the thicker-walled section near the apex. An FMD was introduced at an identical angle, but to a deeper penetration depth (2–4 mm) near the interface of the mucosa and muscularis propria. Sets of infusions were conducted at 50 and 100 μL/min. The higher flow rate experimental set was conducted to determine if there would be any increase in fluid reflux out of the tissue. Three infusions at each flow rate were administered within two bladders for 5, 10, and 15 minutes (N = 2).

Following the completion of both sets of infusions, the bladder tissue was attached to a styrofoam sheet and immediately submerged in 10% neutral buffered formalin solution for fixation. Following a minimum of 24 hours of fixation, tissues were removed and trimmed for further processing. Tissues were dehydrated in a graded series of aqueous ethanols of increasing ethanol concentration, transitioned to ethanol/xylene, xylene/paraffin, and finally paraffin polymer. These dehydration and embedding procedures were done by a Tissue Tek® VIP® 6 automated tissue processing system (Sakura Finetek USA, Inc., Torrance, CA). Once infiltrated with paraffin polymer, three micron sections were cut, rehydrated, and then stained with hematoxylin-eosin stain, using an automated tissue stainer (Leica Microsystems, Wetzlar, Germany).

Another set of experiments was conducted to determine the SWNH dispersal depth in inflated bladders. An FMD was introduced through the serosa proximal to the bladder apex at an angle of approximately 10° to a depth of 2–4 mm. Infusions were conducted at a flow rate of 50 μL/min for 5, 10, and 15 minutes and repeated in a second bladder (N = 2). Immediately after the set of infusions was completed, the bladder was drained, the infused region excised, and the removed tissue attached to a styrofoam sheet for submersion in 10% neutral buffered formalin solution. Following a minimum of 24 hours of fixation, tissues were removed and cut into thin, cross-sectional strips before being photographed with a Canon EOS Rebel T1i/EOS 500D camera (Canon USA, Lake Success, NY).

2.4 Laser Irradiation of Infused SWNHs

Experiments were conducted to test laser heating of infused SWNHs in the bladder wall using a 1064 nm CW diode-pumped fiber laser (IPG Photonics, Oxford, MA). The first experimental set was designed to determine the heating differences produced by laser irradiation of a SWNH perfused area of the bladder wall versus a non-infused control. A collimated laser beam with a 5 mm width was used to irradiate the surface of the inflated bladder's serosal layer. Laser energy was delivered at an irradiance of 0.95 W/cm^2 for 40 seconds. Irradiation of the SWNH perfused tissue was conducted at the center of the visually detectable perfused area. Irradiation of the non-infused tissue was conducted at a similar anatomical location on the bladder wall approximately 1 cm away from the edge of the distinguishable nanoparticle perfused region. During irradiation, temperature distribution across the bladder's surface was recorded by an infrared thermal camera at 60 Hz (Thermovision A40, FLIR Systems, Wilsonville, OR). This experiment was conducted in three bladders (N=3).

To determine whether the SWNHs efficacy as exogenous chromophores was independent of the Gaussian distribution of the laser beam, experiments were performed with a 1.5 cm beam width offset from the SWNH perfused bladder tissue in two bladders (N = 2). The *ex vivo* bladder was inflated and infused with SWNHs as described previously. The 5 mm collimated laser beam was expanded to a 1.5 cm beam width using an achromatic doublet lens (ThorLabs, Sterling, VA). The laser beam spot was offset from the discernibly perfused tissue such that only a portion of the beam's periphery was irradiating that tissue. The laser irradiance was 1.1 W/cm^2, and thermographs were taken over 40 seconds of laser heating.

3.0 Results

3.1 Dispersal of SWNHs Across the Serosa

The silica FMDs were sufficiently robust to be inserted into the inflated, *ex vivo* bladder wall's serosa and muscularis numerous times without fracturing the FMD or breaching the bladder wall by over-penetration into the lumen. A representative series of time lapse images are shown in Figure 2 A-D.

SWNH area expansion across the serosa was shown to increase at a relatively linear average rate of 0.36 ± 0.08 cm^2/min when infused at 50 μL/min. A graph of the average values across the 15 min experiments is shown in Figure 3.

3.2 Dispersal Depth of Infused SWNHs

FMDs were placed into the urothelium of the bisected bladder repeatedly without sustaining damage. Reflux of fluid escaping the interstitial space by traveling along the FMD's outer surface was dependent on flow rate. Infusions at 50 μL/min produced limited reflux, while infusions at 100 μL/min caused obvious bolus formation and some reflux, which was consistent between infusions. Infusions at 100 μL/min did not demonstrate increased dispersal depth when qualitatively inspected by a trained veterinary pathologist.

A photograph of one set of infusions is shown in Figure 2 E, which demonstrates the pinned bladder and infusion points. Histological sections of infusion regions at the thin-walled neck of the bladder exhibited SWNH dispersal through the urothelium and muscular propria for the 5 and 10 min infusions, and complete penetration throughout the bladder thickness for the 15 min infusion. Sections in thicker tissue near the bladder's apex showed SWNH dispersal through 4–5 mm of the wall's thickness for all infusion timescales, with more uniform and laterally widespread dispersals for longer infusions. Results were consistent between experiments. The SWNHs were washed from the sectioned tissue during the staining process; however, SWNH dispersal in the stained sections was evident by the expansion of the mucosal layer, which correlated highly with the localization of nanoparticles evident in the gross section from the thicker tissue shown in Figure 4 A-C.

Fixed cross-sections from the infusion sites into inflated bladders unanimously exhibited SWNH penetration throughout the thickness of the wall, independent of infusion timescale. This is possibly attributable to the thinner tissue of the inflated bladders. A representative photograph is shown in Figure 4 D.

3.3 Laser Irradiation of Infused SWNHs

The temperature increase of an inflated, *ex vivo* bladder wall irradiated with 1064 nm laser energy (0.95 W/cm^2 for a 40 s duration) was measured at a region infused with SWNHs after a 15 minute infusion (> 3 cm^2 area) and a region without infusion. Calculation of maximum change in temperature was done by averaging the temperature pixel values over a 1 mm diameter circle centered around the pixel of highest temperature. Laser heating of a non-infused area yielded a maximum temperature increase of 3.2 ± 0.6 °C, while the heating

of a SWNH infused area yielded a maximum temperature increase of 19 ± 1.5°C (N = 3). Representative thermographs of these results are shown in Figure 5 A-B.

Experiments utilizing an offset laser spot to heat the edge of the SWNH perfused tissue demonstrated that the significant difference in heating caused by the exogenous chromophores was independent of the Gaussian profile of the laser beam. A representative thermograph of the offset laser spot heating at an irradiance of 1.1 W/cm^2 for 40 seconds is shown in Figure 5 C. A detectable temperature gradient was observed across the laser spot on the tissue correlating with the position of the nanoparticle spot.

4.0 Discussion

The experiments performed in this study demonstrated the ability of small, silica FMDs to quickly deliver a useful volume of SWNHs, which can be subsequently heated with 1064 nm laser energy to hyperthermic temperatures in healthy, *ex vivo* bladders. Experimental results indicated that the SWNHs can be readily delivered into the interstitial space through the FMDs, with significant dispersal across the bladder wall and time-dependent dispersal throughout the wall's thickness. Laser irradiation of the infused SWNHs exhibited significantly increased heating in comparison to non-infused tissue.

A large invasive UCC can be estimated as being 1–2 cm in diameter (assuming a roughly spherical geometry) [20]. This suggests that the largest tumors likely to be treated with this device could be assumed to have an observable surface manifestation on the bladder wall between 1–2 cm^2. If the rate of SWNH area expansion measured in this study would be conserved in the *in vivo* case, FMD infusion of SWNHs should penetrate this large tumor within approximately 5 minutes at a volumetric flow rate of 50 μL/min.

The detectable footprint of infused SWNHs was roughly circular for all the experiments (as shown in Figure 2. The center of this circle was at the mid-length of the FMD's protrusion from the 22 gauge syringe needle, as opposed to the beveled microneedle tip. Reflux along the shaft of an infusion needle is typically observed in applications such as convection-enhanced delivery (CED) [37]. Krauze *et al.* proposed an improvement in CED infusion cannula designs through inclusion of a step change increase in needle diameter some distance from the cannula's tip, which was shown to halt the progression of reflux [38]. That concept is mimicked in the FMD design for bladder tissue, and a similar effect of the reflux stopping at the 22 gauge needle was observed. Once the fluid pocket of reflux around the FMD portion of the design stabilized, the fluid perfused into the surrounding bladder tissue, resulting in the roughly circular footprint with its centroid at approximately the mid-length of the silica shaft protruding from the stainless steel needle.

Laser irradiation of SWNH perfused tissue with a free space laser exhibited the efficacy of the nanoparticles as exogenous chromophores within the bladder wall. The maximum heating difference (averaged over 1 mm) between irradiating perfused and non-perfused tissue was approximately 590%. For many hyperthermic therapies, the heating threshold for quickly causing protein denaturation and tissue coagulation has been shown to be 60°C [13, 39]. The maximum tissue temperature increase in the SWNH-perfused tissue was

approximately 19 °C, a increase in temperature that would fall short of 60°C if conserved in an *in vivo* treatment. However, heating levels can be modulated by varying either the laser irradiance or the concentration of the SWNHs [27, 32]. These findings indicate that SWNHs can aid laser heating of tissue in reaching temperatures inducing rapid hyperthermic tissue damage.

The offset laser spot experiment verified that the increase in heating due to SWNH absorption correlated with the infused region of SWNHs more than the center of the Gaussian beam distribution. This implies that by utilizing the FMD's ability to penetrate the bladder wall, SWNHs can be delivered throughout a target volume to shape the zone of photothermal heating from within deeper bladder layers containing neoplastic tissue. This experiment provides evidence that if the SWNH distribution can be contained within a target volume, laser irradiation should cause selective tissue destruction while preserving healthy tissue. Additionally, the centroid of the heated spot was less than the maximum temperature (both averaged over 1 mm^2) by ~3°C for N = 3 trials, indicating that laser heating of the SWNH permeated tissue needs to be with the center of the beam waist to best leverage the SWNHs.

The authors recognize the potential for FMDs delivering both the SWNHs and laser energy. Delivering SWNHs and laser irradiation through the same delivery channel would allow greater accuracy and control of the photothermal dose; however, the light delivery capabilities of the FMD are being currently developed and therefore not described in this manuscript. For treatment of invasive UCCs, one or more FMDs may be guided into the bladder via the working channel of a cystoscope and placed against a tumor located in the bladder urothelium. Mechanical actuation will cause the FMDs to slide through the channel and penetrate the bladder to a final placement at desirable target positions within an invasive UCC. Delivery of exogenous chromophores to specific tissue regions will allow for a localized, targeted treatment and preservation of surrounding healthy tissues. Laser energy emitted from the FMD tip would induce photothermal damage confined by the spread of the SWNHs. This treatment protocol should enable significantly reduced unwanted collateral healthy tissue damage while maximizing energy delivery to tumor tissue.

The authors acknowledge several limitations in the current study which constrain the context of our conclusions. First, all experiments were performed on *ex vivo* tissue, which is not perfused by blood. Blood perfusion may have a significant effect on the dispersion properties of the nanoparticles during infusion. Additionally, blood perfusion will likely affect the thermal convection and thermal localization properties during laser irradiation *in vivo*. A second limitation is the use of healthy bladder tissue for experimentation. The mechanics of injection, dispersion, absorption, and thermal response within invasive carcinomas may be very different from normal bladder tissue. These differences will be examined in future studies.

The FMD can potentially deliver a variety of fluid agents or pharmaceuticals in addition to the specific parameters used in this study. Other wavelengths within the near-infrared region associated with high tissue penetration could be used in conjunction with the SWNHs, such as 800 μm. The fluid delivery method outlined could be used to deliver

other nanoparticles in solution or alternatively be used to deliver adjunctive, local treatments such as chemotherapy or photodynamic therapy. This versatile, enabling technology could be useful for a wide variety of treatment options in addition to the therapeutic concept outlined in the above experiments.

Acknowledgments

The authors would like to acknowledge the NSF (CBET 1R21CA156078) and NIH (NIH/NCI 1R21CA156078) for their funding of this project. Single-walled carbon nanohorns were generously provided by the Center for Nanophase Materials Sciences (CNMS) at Oak Ridge National Laboratories and sponsored by the Department of Energy, Basic Energy Sciences Division of Scientific User Facilities. Fiberoptic microneedle fabrication methods and applications are described in US 13/203,800 and PCT/US2012/026,968, which are managed by the Virginia Tech Intellectual Properties Group.

The authors would like to acknowledge the National Science Foundation and the National Institutes of Health for their funding of this project.

References

1. Bronk BV, Wilkins RJ, and Regan JD, Thermal enhancement of DNA damage by an alkylating agent in human cells. Biochem Biophys Res Commun, 1973. 52(3): p. 1064–70. [PubMed: 4351044]
2. Quek ML, et al. , Prognostic significance of lymphovascular invasion of bladder cancer treated with radical cystectomy. J Urol, 2005. 174(1): p. 103–6. [PubMed: 15947587]
3. Wong-You-Cheong JJ, et al. , From the archives of the AFIP - Neoplasms of the urinary bladder: Radiologic-pathologic correlation. Radiographics, 2006. 26(2): p. 553–U17. [PubMed: 16549617]
4. Hahn GM, Potential for therapy of drugs and hyperthermia. Cancer Research, 1979. 39(6 Pt 2): p. 2264–8. [PubMed: 87263]
5. Rodel C, et al. , Combined-modality treatment and selective organ preservation in invasive bladder cancer: Long-term results. Journal of Clinical Oncology, 2002. 20(14): p. 3061–3071. [PubMed: 12118019]
6. Bladder Cancer Treatment. 2009 8/21/2009 [cited 2010; Available from: http://www.cancer.gov/cancertopics/pdq/treatment/bladder/Patient/page4.
7. Thrasher JB and Crawford ED, Current management of invasive and metastatic transitional cell carcinoma of the bladder. J Urol, 1993. 149(5): p. 957–72. [PubMed: 8483247]
8. Hart S, et al. , Quality of life after radical cystectomy for bladder cancer in patients with an ileal conduit, cutaneous or urethral kock pouch. The Journal of urology, 1999. 162(1): p. 77–81. [PubMed: 10379744]
9. Stein JP, et al. , Radical cystectomy in the treatment of invasive bladder cancer: long-term results in 1,054 patients. Journal of clinical oncology : official journal of the American Society of Clinical Oncology, 2001. 19(3): p. 666–75. [PubMed: 11157016]
10. Syed HA, et al. , Holmium : YAG laser treatment of recurrent superficial bladder carcinoma: Initial clinical experience. Journal of Endourology, 2001. 15(6): p. 625–627. [PubMed: 11552789]
11. Larizgoitia I and Pons JMV, A systematic review of the clinical efficacy and effectiveness of the holmium : YAG laser in urology. Bju International, 1999. 84(1): p. 1–9.
12. Soler-Martinez J, et al. , Holmium laser treatment for low grade, low stage, Noninvasive bladder cancer with local anesthesia and early instillation of mitomycin C. Journal of Urology, 2007. 178(6): p. 2337–2339. [PubMed: 17936805]
13. Pietrow PK and Smith JA Jr., Laser treatment for invasive and noninvasive carcinoma of the bladder. Journal of endourology / Endourological Society, 2001. 15(4): p. 415–8; discussion 425–6.
14. Hruby GW, et al. , Transurethral bladder cryoablation in the porcine model. Journal of Urology, 2008. 179(4): p. 365–365. [PubMed: 18006007]

15. Sternberg CN, et al. , Chemotherapy for bladder cancer: treatment guidelines for neoadjuvant chemotherapy, bladder preservation, adjuvant chemotherapy, and metastatic cancer. Urology, 2007. 69(1 Suppl): p. 62–79. [PubMed: 17280909]
16. Malkowicz SB, et al. , Muscle-invasive urothelial carcinoma of the bladder. Urology, 2007. 69(1 Suppl): p. 3–16.
17. Fedeli U, Fedewa SA, and Ward EM, Treatment of muscle invasive bladder cancer: evidence from the National Cancer Database, 2003 to 2007. The Journal of urology, 2011. 185(1): p. 72–8. [PubMed: 21074192]
18. Phull JS, Modern transurethral resection in the management of superficial bladder tumors. British journal of medical & surgical urology, 2011. 4(3): p. 91.
19. Kramer MW, et al. , Current evidence for transurethral laser therapy of non-muscle invasive bladder cancer. World J Urol, 2011.
20. Johnson DE, Use of the Holmium-Yag (Ho Yag) Laser for Treatment of Superficial Bladder-Carcinoma. Lasers in Surgery and Medicine, 1994. 14(3): p. 213–218. [PubMed: 8208047]
21. Kramer MW, et al. , Current evidence for transurethral laser therapy of non-muscle invasive bladder cancer. World journal of urology, 2011.
22. Das A, Gilling P, and Fraundorfer M, Holmium laser resection of bladder tumors (HoLRBT). Techniques in urology, 1998. 4(1): p. 12–4. [PubMed: 9568769]
23. Ghoneim MA, et al. , Radical cystectomy for carcinoma of the bladder: critical evaluation of the results in 1,026 cases. The Journal of urology, 1997. 158(2): p. 393–9. [PubMed: 9224310]
24. Zhang M, et al. , Fabrication of ZnPc/protein nanohorns for double photodynamic and hyperthermic cancer phototherapy. Proc Natl Acad Sci U S A, 2008. 105(39): p. 14773–8.
25. Iijima S, et al. , Nano-aggregates of single-walled graphitic carbon nano-horns. Chemical Physics Letters, 1999. 309(3–4): p. 165–170.
26. Miyawaki J, et al. , Toxicity of single-walled carbon nanohorns. ACS nano, 2008. 2(2): p. 213–26. [PubMed: 19206621]
27. Whitney JR, et al. , Single Walled Carbon Nanohorns as Photothermal Cancer Agents. Lasers in Surgery and Medicine, 2011. 43(1): p. 43–51. [PubMed: 21254142]
28. Murata K, et al. , Molecular potential structures of heat-treated single-wall carbon nanohorn assemblies. Journal of Physical Chemistry B, 2001. 105(42): p. 10210–10216.
29. Whitney J, et al. , Carbon Nanohorns as Photothermal and Photochemical Laser Cancer Therapeutic Agents. Lasers in Surgery and Medicine, 2009: p. 3–3.
30. Miyako E, et al. , Near-infrared laser-triggered carbon nanohorns for selective elimination of microbes. Nanotechnology, 2007. 18(47).
31. Cheng MD, et al. , Formation studies and controlled production of carbon nanohorns using continuous in situ characterization techniques. Nanotechnology, 2007. 18(18).
32. Sarkar S, et al. , Optical properties of breast tumor phantoms containing carbon nanotubes and nanohorns. Journal of biomedical optics, 2011. 16(5): p. 051304.
33. Sarkar S, et al. , Optical properties of breast tumor phantoms containing carbon nanotubes and nanohorns. Journal of Biomedical Optics, 2011. 16(5).
34. Fisher JW, et al. , Photothermal response of human and murine cancer cells to multiwalled carbon nanotubes after laser irradiation. Cancer Research, 2010. 70(23): p. 9855–64. [PubMed: 21098701]
35. Burke A, et al. , Long-term survival following a single treatment of kidney tumors with multiwalled carbon nanotubes and near-infrared radiation. Proc Natl Acad Sci U S A, 2009. 106(31): p. 12897–902.
36. Whitney JR, et al. , Spatial and temporal measurements of temperature and cell viability in response to nanoparticle-mediated photothermal therapy. Nanomedicine (Lond), 2012.
37. Morrison PF, et al. , Focal delivery during direct infusion to brain: role of flow rate, catheter diameter, and tissue mechanics. The American journal of physiology, 1999. 277(4 Pt 2): p. R1218–29.
38. Krauze MT, et al. , Reflux-free cannula for convection-enhanced high-speed delivery of therapeutic agents - Technical note. Journal of Neurosurgery, 2005. 103(5): p. 923–929. [PubMed: 16304999]

39. Dowlatshahi K, et al. , Stereotactically guided laser therapy of occult breast tumors: work-in-progress report. Archives of surgery, 2000. 135(11): p. 1345–52. [PubMed: 11074894]

Figure 1:
Image of sharp, beveled tip of an FMD. Water is visible inside the hollow bore.

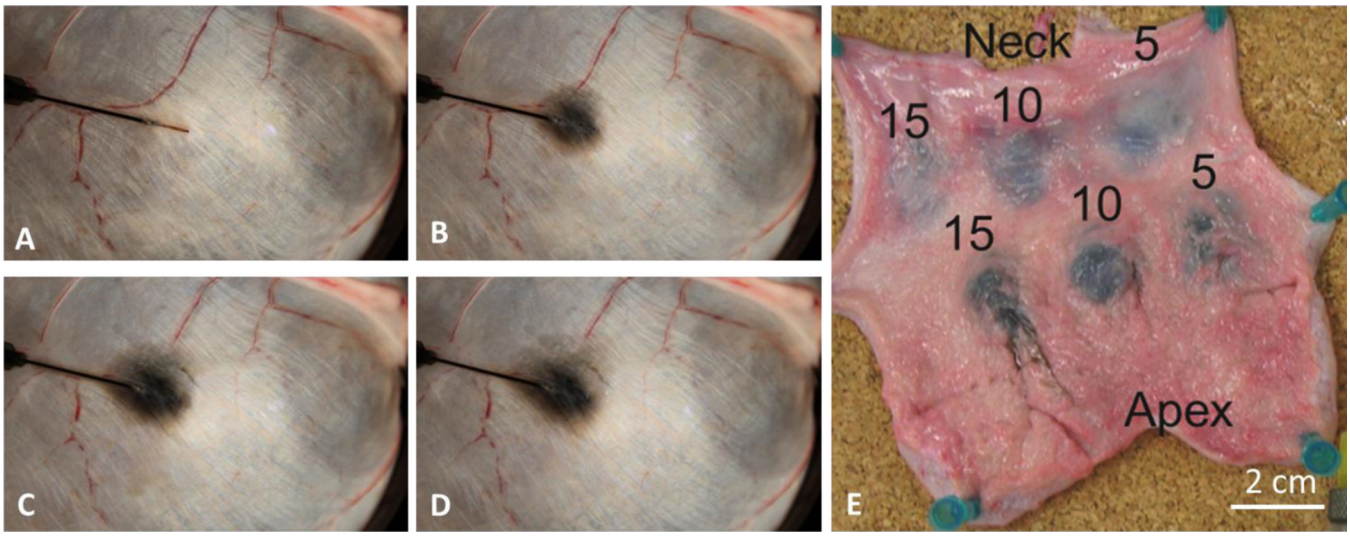

Figure 2:

SWNH infusion through FMD into an *ex vivo* porcine bladder wall. (A) t = 0 min, area = 0 (B) t = 4 min, area = 1.5 cm^2 (C) t = 8 min, area = 2.6 cm^2 (D) t = 12 min, 3.2 cm^2 (E) Two sets of infusions, located proximal to the neck and apex of the bladder are labeled with their infusion times in minutes. The infusion rate was 50 μL/min for the neck infusions and 100 μL/min for the apical infusions.

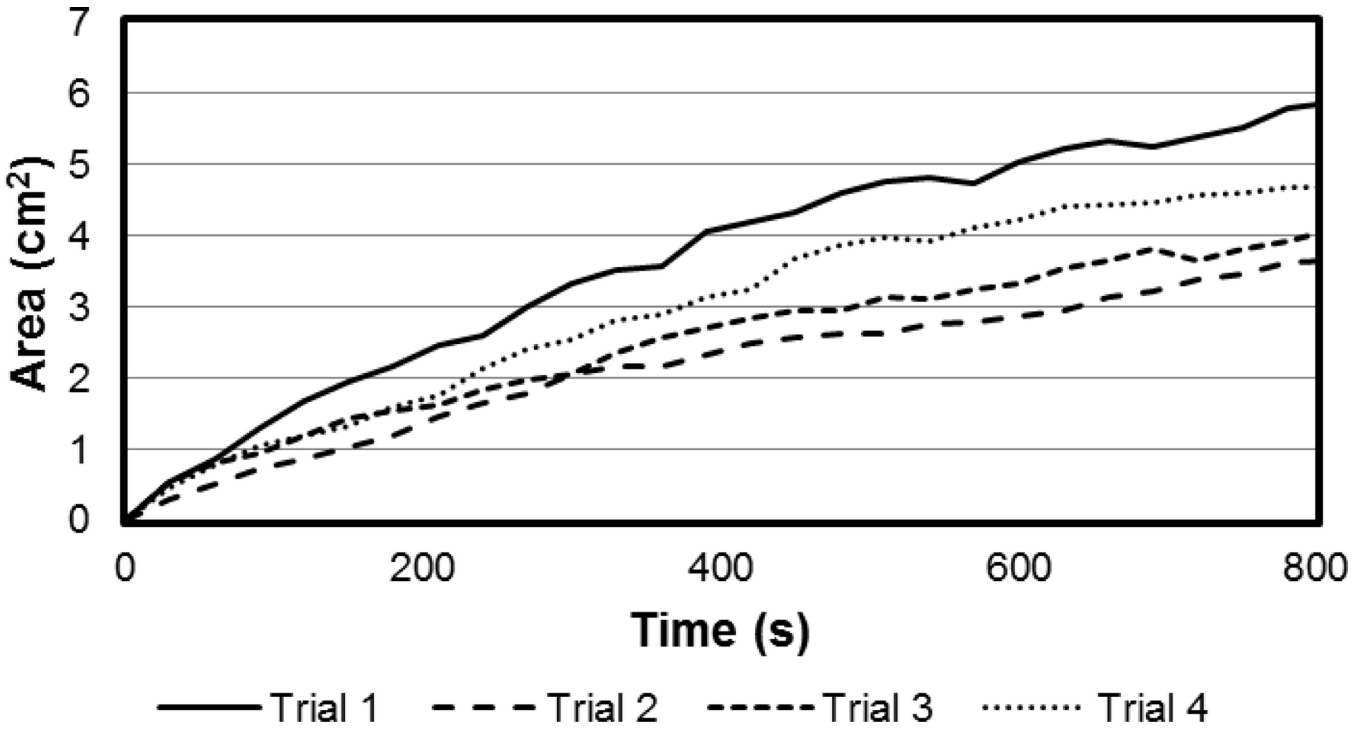

Figure 3:

Area of SWNH dispersal versus time plot of data from image analysis of photographs of the serosa taken every 30 s during SWNH infusion at 50 μL/min into the wall of an inflated bladder. Four trials conducted with identical infusion parameters.

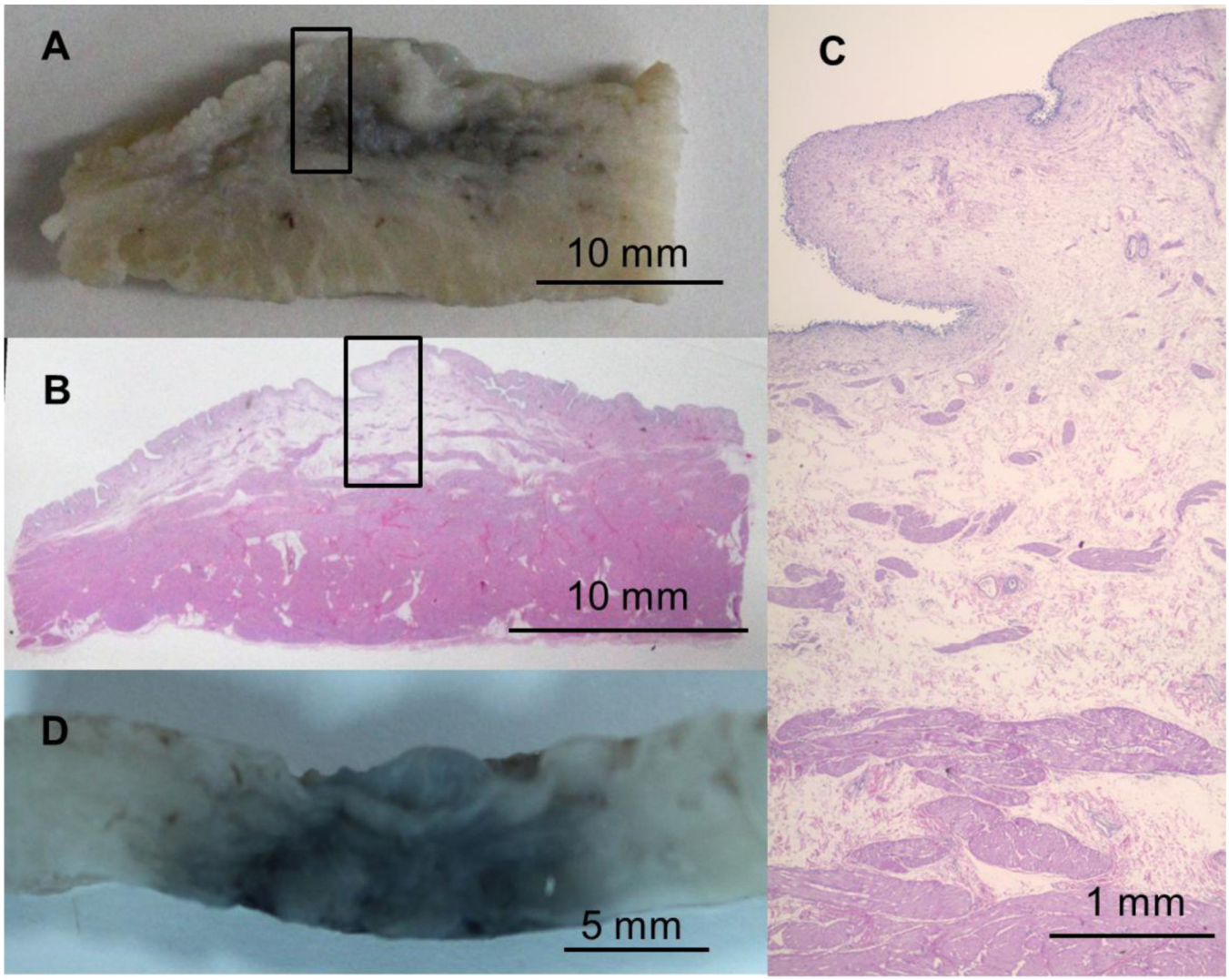

Figure 4:

(A) Gross section of formalin-fixed bladder wall following 5 minute infusion into the neck region of uninflated bladder. (B) Histological section cut directly from the gross section (A). (C) Close view of the stained section (location denoted by black boxes in (A) and (B)) showing expansion of the loose connective tissue in the mucosal layer from fluid expansion caused by SWNH infusion. (D) Gross section of fixed bladder wall following 10 minute infusion into inflated bladder showing SWNHs dispersal throughout the wall's thickness. All tissue is oriented with the urothelial layer upwards.

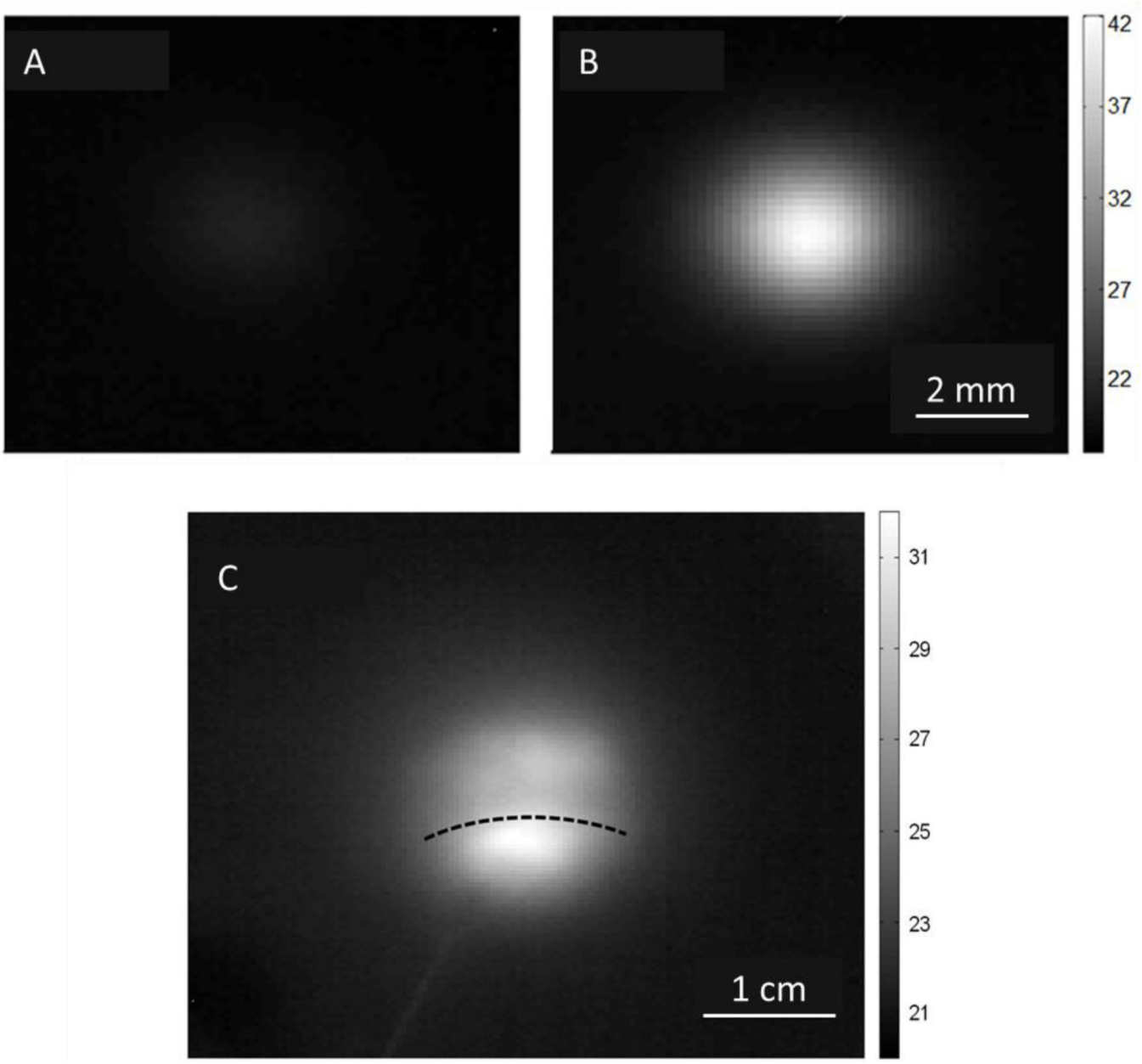

Figure 5:

Thermographs of laser heating bladder tissue in regions: (A) without SWNHs, (B) with SWNHs (A,B have 5 mm beam width) (C) Offset from SWNH dispersal (1.5 cm beam width). The highest temperature correlates with the laser/SWNH overlap. The SWNH dispersal area covers the entire image in (A) and (B). The dotted line in (C) marks the top edge of the SWNH spread. Intensity scale is in Celsius.